ORIGINAL PAPER

A study on the role of BaTiO$_3$ in lithum bis (perfluoroethanesulfonyl)imide-based PVDF-HFP nanocomposites

P. Vickraman · V. Senthilkumar

Abstract Lithium bis(perfluoroethanesulfonyl)imide (BETI; guest species)-based polyvinylidenefluoride-hexafluoropropylene (PVDF-HFP) (host matrix) polymer nanocomposites (PNC) films by loading barium titanate (BaTiO$_3$) as a filler in ascending proportions with plasticizer (mixture of EC+DMC) while keeping host and guest content as constants has been investigated by employing AC impedance, thermal, X-ray diffraction (XRD), phase morphology, and Fourier transform infrared (FTIR) studies. The ionic conductivity measurements on these PNC show that 2.5% BaTiO$_3$-loaded polymer nanocomposites (PNC) showed mitigation in magnitude of the conductivity compared with that of 0 wt.% loaded PNC; but increase in conductivity is noted thereafter with increase in filler content of up to 7.5 wt. %. The higher conductivity is observed for 7.5% filler-loaded membrane. The XRD study identifies suppression of polymer phase associated with (200) plane. The SEM image illustrates inhomogeneity in surface morphologies for PNCs with the filler dispersed. The thermal profile registers the endothermic changes associated with polymer host indicating a varying heat of fusion ΔHm with filler increase. FTIR studies confirm possible interaction between various constituents of the PNCs.

Keywords PVDF-HFP · BaTiO$_3$ · Phase morphology · XRD · DSC

Introduction

Gel-type polymer electrolytes have gotten their potential applications in energy storage devices as a separator cum electrolyte in lithium-ion batteries. From earlier investigations with Vincent et al. [1] to date, the exploration of different types of polymer electrolytes with different polymer [2–8] salts have been explored. With so many shortcomings of the types of polymers employed, it is identified that PVDF host is believed to be a potential host for lithium-ion batteries. However, PVDF being highly crystalline is copolymerized with hexafluoropropylene (HFP) to reduce its crystallinity [9,10] and being able to use it as a potential host in polymer electrolytes. As far as salts are concerned, numerous investigations have been carried out to identify the suitable lithium salts for commercial lithium-ion battery applications, and in this line lithium hexafluoro phosphate has been identified as a commercially viable electrolyte. However, this type of salt also creates certain problems while in use. So the search for newer types of salts are explored, and in this line lithium bis(perfluoroethanesulfonyl)imide (BETI), i.e., LiBETI is identified as one of the salts circumventing certain demerits of LiPF$_6$.LiBETI which may be considered promising for industrial applications due to its larger anion size and higher polarizability which would be effective in terms of the cation transport properties. Barium titanate as a filler is chosen because it exhibits the highest electrolyte uptake, ionic conductivity, electrochemical stability, and better compatibility with lithium metal among the inert fillers [11] SiO$_2$, Al$_2$O$_3$, and TiO$_2$ being studied. Thus, the polyvinylidenefluoride (PVDF)-HFP is the best host that can accommodate within its matrix the lithium BETI salt as a best guest [12], Ethylene carbonate and dimethyl carbonate (DMC) as a softening additives and BaTiO$_3$ as filler have been selected. Yamamoto and coworkers [13] also reported the enhanced conductivity and the decrease of interfacial resistance between the lithium anode and polymer

P. Vickraman (✉) · V. Senthilkumar
Department of Physics, Gandhigram Rural University,
Gandhigram 624302, India
e-mail: vrsvickraman@yahoo.com

electrolyte by the addition of BaTiO₃. Li et al. [14] studied the cycling performance of PEO-based composite electrolytes with three fillers, $BaTiO_3$, TiO_2, Al_2O_3, SiO_2, and $Li(CF_3SO_3)_2$ N and as a salt and found that $BaTiO_3$ as filler improved interfacial stability between the electrolyte and electrode. Based on the literature available, no work has been explored in the host selected (PVDF-HFP) with the salt chosen LiBETI and with the filler selected ($BaTiO_3$). So the present work is focused on preparation, characterization, and evaluation of $BaTiO_3$-loaded lithium bis(perfluoroethanesulfonyl)imide-based PVDF-HFP to optimize ionic conductivity by varying filler-plasticizer ratio while keeping host and guest content as constant.

Materials and instrumentations

Materials

PVDF (mol. wt. 5.34×10^5) with 12 mol% of HFP was obtained from Solvay Solexis S.p.A., Italy. The plasticizers ethylene carbonate (EC) and DMC were obtained from Aldrich, USA and used as such. The filler barium titanate (IV) ($BaTiO_3$) powder with 99% of purity was purchased from Fluka, USA. The solvent tetrahydrofuran, HPLC grade was purchased from E. Merck, India, and used without further purification. The lithium BETI with a molecular weight of 387.13 was purchased from Fluka, USA, and used as received. PNC membranes were prepared according to the composition shown in Table 1 by solution casting technique.

Instrumentations

Ionic conductivities of the membranes were measured by alternating current (AC) impedance spectroscopy in the frequency range 42 Hz–5 MHz by using a HIOKI 3532-50 LCR Hitester. The conductivity cell consists of two circular stainless steel blocking electrodes (SS/SCPE/SS) of 1 cm² cross-sectional area. The Fourier transform infrared (FTIR) spectrum was recorded between 4,000 and 400 cm⁻¹ in the transmittance mode using JASCO 460Plus IR spectrophotometer with a 4 cm⁻¹ resolution. Morphological features of the membranes were examined using a Hitachi Model S-3000H scanning electron microscope. Differential scanning calorimetric traces were recorded using a METTLER instrument. The thermal events were recorded in nitrogen between 0 to 300 °C at a heating rate of 10°C/min. X-ray diffraction measurements were recorded on a PAN anlytical X-ray diffractometer with Cu Kα1 (λ=1.5418Å) between scattering angles of 10–80°.

Results and discussion

Ac impedance studies

The ionic conductivity of PVDF-HFP-based electrolytes is measured for various filler-plasticizer ratio (Table 2). The ionic conductivities of membranes are calculated from the following equation

$$\sigma = \frac{l}{R_b \pi r^2}$$

Where, l and r represent thickness and radius of the sample, respectively. R_b is the bulk resistance obtained from AC impedance plot. The temperature dependence of ionic conductivity and their variations with varying filler contents in the PVDF-HFP-based electrolytes are shown in Fig. 1a, b. The quantitative description of conductivity is given by relation $\sigma_i = n_i e z$. This is the conductivity performance as it is being related to the mobility and concentration of lithium ions. If the concentration is maintained constant, then the mobility must account for the conductivity. Here, mobility is constrained by the introduction of a 2.5 wt.% filler particles. These particles generate polarization due to Li⁺ cations being trapped for a short time (blocking effect) in a localized electric field that might have inhibited flexibility of the polymer host and did not provide pathways for ion migration. This might be the cause for the sudden decrease

Table 1 Composition of polymer nanocomposites

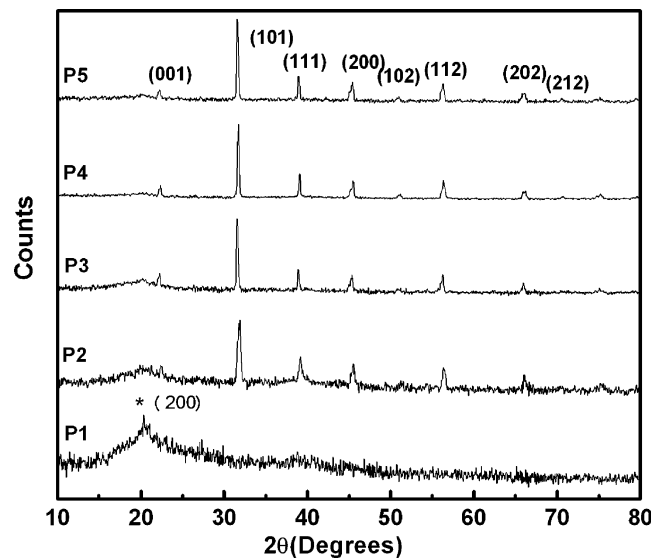| Sample	PVDF-HFP (wt.%)	Plasticizer		LiBETI (wt.%)	BaTiO₃ (wt.%)
		EC (wt.%)	DMC (wt.%)		
P1	30	32.50	32.50	5	00.00
P2	30	31.25	31.25	5	02.50
P3	30	30.00	30.00	5	05.00
P4	30	28.75	28.75	5	07.50
P5	30	27.50	27.50	5	10.00

Table 2 Temperature dependence on ionic conductivity for PNC

Samples	Filler (wt.%)	Ionic conductivity(10^{-3} Scm^{-1})		
		30°C	40°C	50°C
P1	0	0.77	0.76	0.65
P2	2.5	0.44	0.36	0.35
P3	5.0	1.15	1.22	1.04
P4	7.5	1.26	1.27	1.65
P5	10	0.84	0.80	1.06

Fig. 2 X-ray diffraction patterns of lithium ion conducting PNC

in magnitude of conductivity. This will confirm polymer–filler interaction, and further addition might have caused imbalance in the continuum of the particulate mass relaxation due to the spontaneous polarization (space charge effect) that guided the ion migration which then facilitates an improved conductivity profile of up to 7.5 wt. %. In numerous composite systems, the space charge and blocking effects are operative and have been observed and reported [15–17]. The same trend of ionic conductivity variations were reported by other workers [18,19]. In the particulate mass aggregation at 10 wt.%, no plastization effect of filler on polymer is seen as it is causing sudden decrement of conductivity and rather, no flexibility of polymer backbone resulted.

X-ray diffractogram

X-ray diffraction analysis is performed to examine the crystalline nature of the polymer host. Figure 2 shows XRD patterns of the membranes P1, P2, P3, P4, and P5 which respectively correspond to 0, 2.5, 5, 7.5, and 10 wt.% filler. For the filler-free membrane P1, it is observed that $2\theta =$

20.47°, referring to (200) plane of PVDF [20], corresponds to the α phase of VdF crystal found in the present study. The incorporation of filler 2.5 wt.% suppresses the (200) plane of PVDF as shown in XRD pattern which represents the interaction between filler and the polymer, and emergence of (hkl) planes refer to the presence of BaTiO$_3$ from the sample P2. The intensity variation of peaks is found to be proportional to the particulate mass content being observed. This is also inferred that α phase of PVDF happens to be an amorphous phase which might have been polarized for a short time while ion migration constricts and thus resulted in the decrease in magnitude of conductivity in P2. Further addition of filler facilitates ion migration after recovering from the short relaxation caused by the
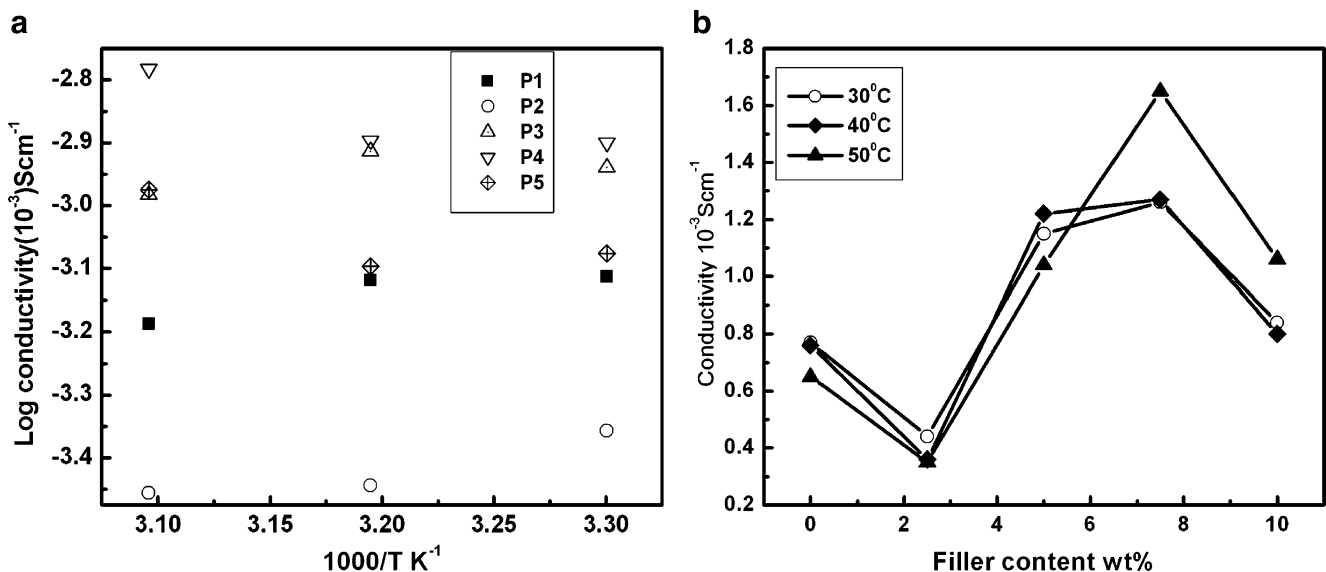
Fig. 1 a The temperature dependence on ionic conductivity, and b variation of ionic conductivity with varying filler contents

polarization of filler with polymer and is therefore accounted for the increase in conductivity of up to P4 and beyond from which it is shown that filler–filler interaction may be dominating the fall reflected in the conductivity and as such, plastization effect on polymer is no longer possible.

Fourier transform infrared studies

In the present study, the IR spectroscopy is used to establish the interaction between polymer, salt, plasticizer, and filler. Such interaction can induce changes in the vibrational modes of the atoms or molecules in the material which in turn changes the physical and chemical properties of the constituents of the complex. IR spectroscopy of polymer is based on the excitation of polymer vibrations by absorption of photons in the IR region of the spectrum of electromagnetic radiation. Figure 3a represents the vibrational bands of pure samples. The very importance of understanding the molecular interactions can be well understood only in the fingerprinting region. Thus, it is mainly the concern in the present study because only in this region that a lot of bending vibrations which correspond to the degree of complexation of the various constituents can be understood. The characteristic vibrational bands 532, 761, and 975 cm^{-1} correspond to the α phase crystal of PVdF [21]; the bands 488 and 841 cm^{-1}, respectively, correspond to β and γ phases of VdF crystals [22], and bands at 841 and 975 which correspond to amorphous phase of PVDF-HFP are identified, i.e., 761, 841, and 975 cm^{-1}, respectively, refer to CF_2 scissoring C–C–C skeletal bending of C(F)–C(H)–C (F), CH_2 rocking, C–C symmetric stretching, and C–C–C

skeletal bending of C(F)–C(H)–C(F) and CH_2 twisting vibrations of the α phase of VdF crystal, and 615 cm^{-1} correspond to symmetrical stretching mode of C–F wagging mode, 1183 and 1071 cm^{-1} correspond to symmetrical stretching mode of which CF_2 and CF_3 groupings [23] are found. The wave numbers associated with the ascending loading of filler asserts the complexation of PVDF is shown in Fig. 3b, c. The PVDF compatibility with EC evidently shows that it is not fully miscible with EC which was proven [24] due to the reappearance of some bands of pure EC at 1453 and 1482 cm^{-1} corresponding to C–H bending vibration and 1555, 1638, 1964 cm^{-1} corresponding to C=O carbonyl band in the spectral region. The nonlinear increase and decrease of the ionic conductivity for a fixed temperature with increase in filler is well substantiated while observing reduction in intensity of the band and their complete absence at 7.5 wt.%. Their reappearance at 10 wt.% suggests that filler–filler interaction is dominant than filler–polymer interaction.

Thermal studies

The differential scanning calorimetric technique which illustrates the thermal history of polymers such as melting temperature, glass transition temperature, heat of fusion, degradation, etc. The present study is carried out to understand the molecular history of membrane from 0 to 300 °C at the scanning rate of 10 °C/min (Fig. 4). The thermal behavior of this piezo-electric polymer filled with ferroelectric filler content is found to be showing very interesting thermal history in the range recorded and investigate the change in the polymer crystalline phases
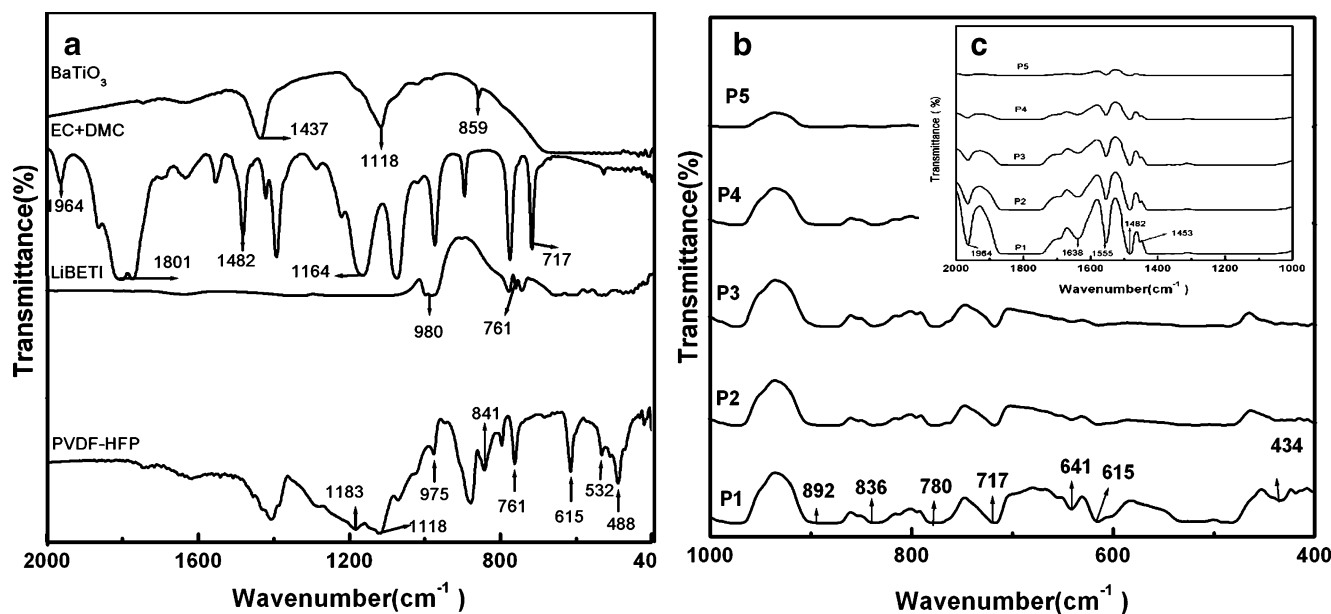
Fig. 3 a FTIR spectra of pure samples, b FTIR spectra of P1–P5 400–1,000 cm^{-1}, and c FTIR spectra of P1–P5 1,000–2,000 cm^{-1}
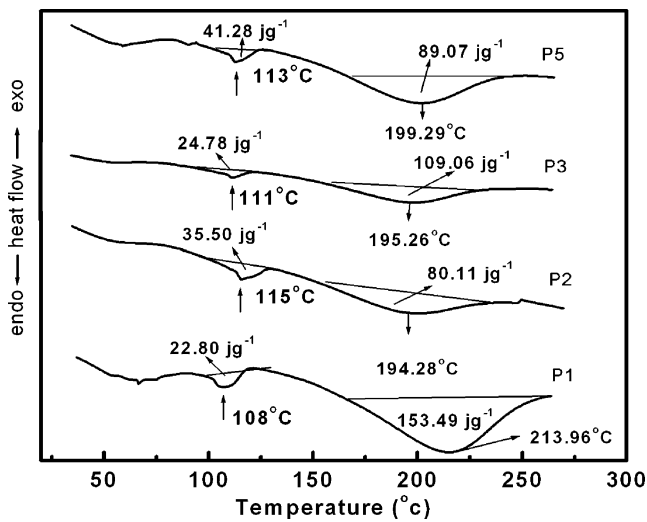
Fig. 4 Differential scanning calorimetric traces of PNCs

which all samples show very prominent two endothermic events with the corresponding variations in heat of fusion (ΔH_m). The ΔH_m changes for a broad endothermic event at 153.49 °C in the filler-free membrane drastically showed its reduction for the 2.5 wt.% to 80 J/g, and for P3 it shoots up to 109 J/kg and in the higher content of 10 wt.% filler

loaded and is then reduced down to 89 J/g. This broad endothermic fluctuation might have been caused by phase transformation of barium titanate as it is temperature dependent [25] and because of its high polarization which disrupts the orientation of the polymer backbone. These nonlinear thermal fluctuations of the sample events are also well seen in ionic conductivity measurements, i.e., increase in the filler content highly disrupts the swollen–gel polymer matrix. As far as the crystalline phases of PVdF are concerned, it is known to have four crystalline forms [25]. The equilibrium melting point of the α [II] crystal form is 213 °C, and the phase change is associated with the relaxation process which pronounced at high temperature that 108 °C corresponds to β crystal form. The thermal studies confirm thermal history of polymer–filler interaction.

Phase morphological studies

Phase morphological natures of the PNCs have been presented in Fig. 5. The filler-free membrane shows homogeneity in surface which is altered due to the addition of 2.5 wt.% showing an unevenly sprouted particulates. Further addition develops the inhomogenity of dispersions facilitating filler pathways for ion migration. The profile of
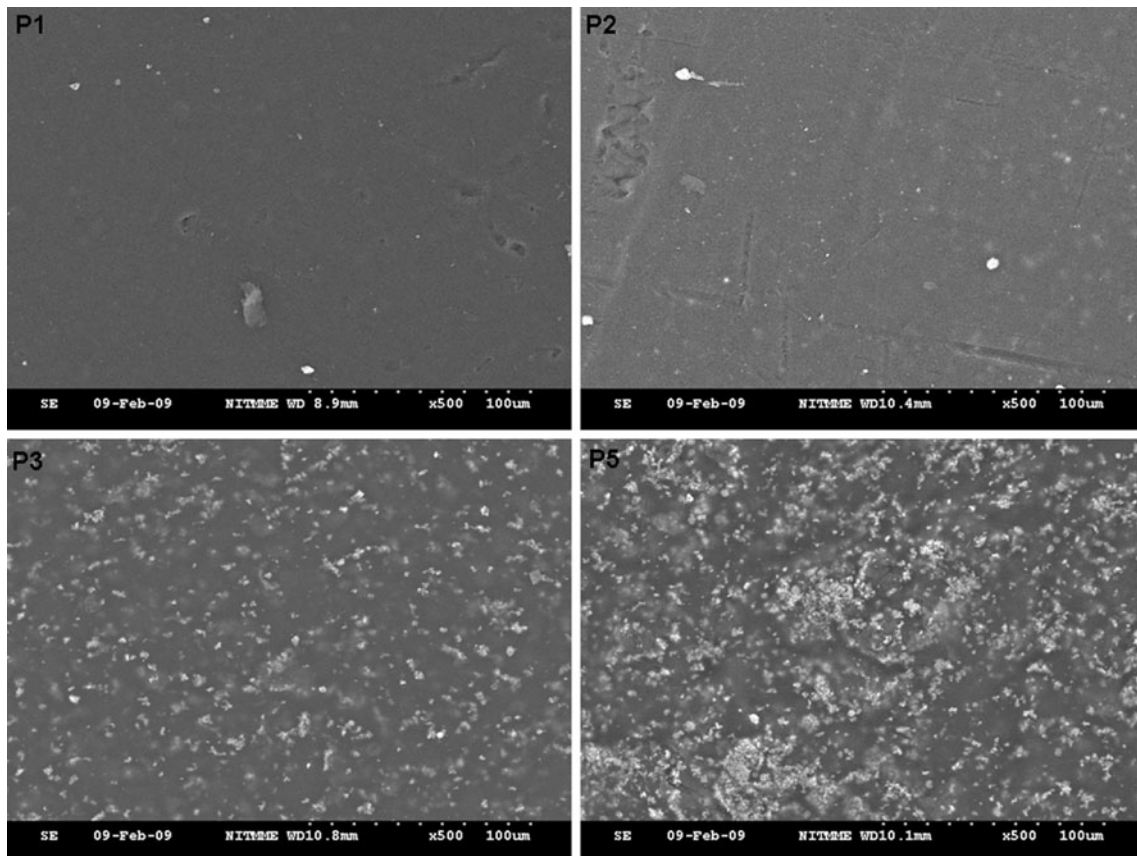

Fig. 5 SEM images of P1–P5

inhomogenity of the surface morphology which grows dominantly with ascending filler content reached to a concrete agglomeration which might have been caused by the closing of voids for ionic migration and is well reflected in impedance XRD and also in thermal studies.

Conclusion

Optimization of filler dispersion in host–guest matrix is evidently proven. In this study, it reveals the temperature dependence of PNC. The pore-like appearances formed seemed to show highly developed voids which might have been caused by the highly polarized effect of the metal ceramic. FTIR analysis identifies 7.5 wt.% filler-added system exhibiting very good complexation with other constituents and supports the enhanced ionic conductivity. The thermal profile of PVDF host matrix with free and loaded filler content profile shows the phase transformation of polymer and also the high polarization effect of BaTiO$_3$. Thus, nature and filler content plays a very delicate role to decide upon the ionic conductivity of the PNCs being realized in this study.

References

1. Mac Callum JR, Vincent CA (1979) Polymer electrolyte reviews 1 and 2. Elsevier, New York
2. Nagatomo T, Ichikawa C, Omato O (1987) All-plastic batteries with polyacetylene electrodes. J Electrochem Soc 134:305–308
3. Michot T, Nishimoto A, Watanabe M (2000) Electrochemical properties of polymer gel electrolytes based on poly(vinylidene fluoride) copolymer and homopolymer. Electrochim Acta 45:1347–1360
4. Croce F, Dautzemberg G, Passerini S, Appetecchi GB, Scrosati B (1994) Synthesis and characterization of highly conducting gel electrolytes. Electrochim Acta 39:2187–2194
5. Abraham KM, Alamgir M (1990) Li+-conductive solid polymer electrolytes with liquid-like conductivity. J Electrochem Soc 137:1657–1658
6. Sukeshini AM, Nishimoto A, Watanabe M (1996) Transport and electrochemical characterization of plasticized poly(vinyl chloride) solid electrolytes. Solid State Ionics 86–88:385
7. Appetecchi GB, Dautzenberg G, Scrosati B (1996) A new class of advanced polymer electrolytes and their relevance in plastic-like, rechargeable lithium batteries. J Electrochem Soc 143:6–12
8. Kim HT, Kim KB, Kim SW, Park JK (2000) Li-ion polymer battery based on phase-separated gel polymer electrolyte. Electrochim Acta 45:4001–4007
9. Quartarone E, Brusa M, Mustarelli P, Magistris CT (1998) Preparation and characterization of fluorinated hybrid electrolytes. Electrochim Acta 44:677–681
10. Capiglia C, Saito Y, Yamamoto H, Kageyama H, Mustarelli P (2000) Transport properties and microstructure of gel polymer electrolytes. Electrochim Acta 45:1341–1345
11. Raghavan P, Zhao X, Kim J-K, Manuel J, Chauhan GS, Ahn J-H, Nah C (2006) Ionic conductivity and electrochemical properties of nanocomposite polymer electrolytes based on electrospun poly (vinylidene fluoride-co-hexafluoropropylene) with nano-sized ceramic fillers. Electrochim Acta 54:228–234
12. Capglia C, Saito Y, Kataoka H, Kodama T, Quartarone E, Mustarelli P (2000) Structure and transport properties of polymer gel electrolytes based on PVdF-HFP and LiN(C$_2$F$_5$SO$_2$)$_2$. Solid State Ionics 131:291–299
13. Sun HY, Takeda Y, Imanishi N, Yamamoto O, Sohn H (2000) Ferroelectric materials as a ceramic filler in solid composite polyethylene oxide-based electrolytes. J Electrochem Soc 147:2462–2467
14. Li Q, Takeda Y, Imanishi N, Yang J, Sun JY, Yamamoto O (2001) Cycling performances and interfacial properties of a Li/PEO-Li (CF3SO2)2N-ceramic filler/LiNi0.8Co0.2O2 cell. J Power Sources 97–98:795–797
15. Agrawal RC, Gupta RK (1999) Detailed investigation of the temperature dependence of ionic transport parameters of a new composite electrolyte system (1−×) (0.75AgI: 0.25AgCl): xSnO2. J Mater Sci 34:1131–1162
16. Mikrajuddin A, Shi G, Okuyama K (2000) Electrical conduction in insulator particle—solid-state ionic and conducting particle-insulator matrix composites a unified theory. J Electrochem Soc 147:3157–3165
17. Knauth P (2000) Ionic conductor composites: theory and materials. J Electro Ceram 5:111–125
18. Hasegawa R, Takahashi Y, Chatani Y, Tadokoro H (1972) Joint Committee on Powder Diffraction Standards (JCPDS) card no421651. Polym. J. 3, 600
19. Agnihotry SA, Ahmad S, Gupta D, Ahmad S (2004) Composite gel electrolytes based on poly(methylmethacrylate) and hydrophilic fumed silica. Electrochim Acta 49:2343–2349
20. Ahmad S, Deepa M, Agnihotry SA (2008) Effect of salts on the fumed silica-based composite polymer electrolytes. Sol Energy Mater Sol Cells 92:184–189
21. Marand L, Stein RS, Stack GM (1988) Isothermal crystallization of poly(vinylidene fluoride) in the presence of high static electric fields. I. Primary nucleation phenomenon. J Polymer Phys Sci 26:1361–1366
22. Quist AS, Bates JB, Boyed GE (1971) J Chem Phys 54:4896
23. Aravindan V, Vickraman P, Premkumar T (2008) Polyvinylidene fluoride–hexafluoropropylene (PVdF–HFP)-based composite polymer electrolyte containing LiPF3(CF3CF2)3. J Non-cryst Solids 354:3451–3457
24. Wang Z, Haung B, Huang H, Chen L, Xue R, Wang F (1996) Investigation of the position of Li+ions in a polyacrylonitrile-based electrolyte by Raman and infrared spectroscopy. Electrochim Acta 41:1443–1446
25. Dohany JE, Humphrey JS (1989) In: Kroschwitz JI (ed) Encyclopedia of polymer science and engineering, Vol 17, 2nd edn. Wiley, New York, p 532